materials

MDPI

Article

Performance Assessment of Carbon Dioxide Sequestration in Cement Composites with a Granulation Technique

Jeong-Bae Lee [1], Jun-Hyeong Kim [2], Byeong-Gi Min [1,*] and Byeong-Hun Woo [3,*]

[1] Department of Civil Engineering, Daejin University, 1007 Hoguk-ro, Pocheon-si 11159, Republic of Korea; jblee@daejin.ac.kr
[2] Geomarble-Labs, 6-26, Jeonggeum-ro 162beon-gil, Gasan-myeon, Pocheon-si 11167, Republic of Korea; bspring@nate.com
[3] Civil and Environmental Engineering Department, Hanyang University, Jaesung Civil Engineering Building, 222 Wangsimni-ro, Seongdong Gu, Seoul 04763, Republic of Korea
* Correspondence: garakmin@seoul.go.kr (B.-G.M.); dimon123@hanyang.ac.kr (B.-H.W.); Tel.: +82-2-2220-4323 (B.-H.W.)

Abstract: The cement industry emits a significant amount of carbon dioxide (CO_2). Therefore, the cement industry should recycle the emitted CO_2. However, sequestration by carbonation in cement composites absorbs a very small amount of CO_2. Therefore, a direct way of achieving this is to improve the absorption performance of CO_2 in cement composites. In this study, to improve absorption, unlike in existing studies, a granulation technique was applied, and the material used was calcium hydroxide (CH). In addition, granulated CH was coated to prevent a reaction during the curing of cement paste. The coated CH granule (CCHG) was applied to 5% of the cement weight as an additive material, and the specimens were cured for 91 days to wait for the coating of CCHG to fully phase-change. The experiment of CO_2 absorption showed an unexpected result, where the use of blast furnace slag (BFS) and fly ash (FA) had a negative effect on CO_2 sequestration. This was because BFS and FA had a filler effect in the cement matrix, and the filler effect caused the blocking of the path of CO_2. In addition, BFS and FA are well-known pozzolanic materials; the pozzolan reaction caused a reduction in the amount of CH because the pozzolan reaction consumed the CH to produce a calcium silicate hydrate. Therefore, the pozzolan reaction also had a negative effect on the CO_2 sequestration performance combined with the filler effect. The CO_2 sequestration efficiency was decreased between ordinary cement paste and BFS-applied specimens by 45.45%. In addition, compared to cases of ordinary cement paste and FA-applied specimens, the CO_2 sequestration performance was decreased by 63.64%. Comprehensively, CO_2 sequestration performance depends on the porosity and amount of CH.

Keywords: carbon dioxide; sequestration; granulation; coating; cement composites

check for updates

Citation: Lee, J.-B.; Kim, J.-H.; Min, B.-G.; Woo, B.-H. Performance Assessment of Carbon Dioxide Sequestration in Cement Composites with a Granulation Technique. *Materials* **2024**, *17*, 53. https://doi.org/10.3390/ma17010053

Academic Editors: Federica Raganati and Paola Ammendola

Received: 24 November 2023
Revised: 11 December 2023
Accepted: 18 December 2023
Published: 22 December 2023

1. Introduction

The cement industry emits a large amount of carbon dioxide (CO_2). The amount of CO_2 emission from the cement industry accounts for approximately 7% of global emissions and is the second largest source of carbon emissions worldwide [1]. Due to its large amount of CO_2 emissions, the cement industry has a responsibility to reduce CO_2. It is well known that cement composites react with CO_2 and generate calcium carbonate (CC) following the process of Equation (1).

$$Ca(OH)_2 + CO_2 \rightarrow CaCO_3 + H_2O \tag{1}$$

Cement composites consume calcium hydroxide (CH) and generate the CC. With this process, cement composites absorb almost 70% of the CO_2 that is generated by the production of cement during their service life [2]. However, this process takes a long time to absorb a sufficient amount of CO_2 [2]. The earth is suffering from the effects of greenhouse gases, therefore, greenhouse gases need to be reduced, especially in the cement industry [3]. Therefore, the acceleration of CO_2 absorption using cement composites with some special material needs to be studied.

Skocek et al. [4] focused on the mechanism of the reactions between hardened cement paste and CO_2. The special point of Skocek et al. [4] was the use of recycled concrete. The results indicated that the carbonated paste from recycled concrete could be used as a supplementary cementitious material when the paste was ground into a fine powder [4]. In addition, the capturing performance of CO_2 was increased, and the saving potential was 114.5 g of CO_2 per 100 g of the carbonated paste [4]. A similar study was performed by Huntzinger et al. [5], who confirmed CO_2 sequestration performance using cement kiln dust. The main components of the cement kiln dust were CaO and SiO_2, and the minor components were MgO and K_2O. As expected from the results of Huntzinger et al. [5], CaO was the main reactive component of CO_2. However, contrary to their expectations based on the demonstrated factor of the CO_2 reaction with MgO [6], the reaction between K_2O and CO_2 was larger than that of MgO and CO_2 [5]. Taking into account the unexpected results from Huntzinger et al. [5], cement kiln dust could be used as a CO_2-capturing material. Eloneva et al. [7] performed a CO_2-fixing experiment using blast furnace slag. This experiment showed the potential of blast furnace slag as a suitable material for fixing CO_2 [7]. On the other hand, a natural material was also studied as a sequestrating material for CO_2: red mud [6]. The main component of the red mud was SiO_2, and its content of CaO was almost 2 to 8%, which is a relatively smaller amount than the recycled material or byproduct [6]. Due to the composition of the red mud, it was expected that the CO_2 capturing performance would not be good. However, Na_2O also had a reactive characteristic with CO_2, therefore, red mud had enough potential to capture CO_2 [6].

Another method of using cementitious waste is to use a byproduct such as fly or bottom ash. In particular, the creation of municipal solid waste (MSW)-incinerated bottom ash (MSWIBA) is a problem that has been highlighted recently. Bangkok has increased MSW generation by 493%, Ha-Noi has increased it by 492%, Jakarta has increased it by 506%, and Wuhan has increased it by 600%, respectively, because of the COVID-19 pandemic [8]. In addition, MSWIBA cannot be reused, because the materials are incinerated [6] and it contains toxic heavy metals [9]. Therefore, MSWIBA is considered a material that is difficult to treat. However, Rendek et al. [10] found that MSWIBA could capture CO_2. MSWIBA has a sufficient amount of CaO, MgO, and Na_2O, therefore, these components react with CO_2, and then the CO_2 can be fixed [10]. In addition to bottom ash, lightweight fine aggregates can also be considered, like MSWIBA. Luo et al. [11] investigated CO_2 absorption using zeolite. Since zeolite has pores, CO_2 absorption was confirmed, and CH consumption was detected at the same time. In another case, Gupta et al. [12] investigated carbon sequestration performance using lightweight foamed cement mortar. Gupta et al. [12] added biochar particles as an additional material for the fine aggregate, rather than a replacement material. Biochar and the foamed cement matrix include a much higher ratio of pores than ordinary cement mortar, therefore, the CO_2-passing paths were more abundant inside the hardened cement paste than in the ordinary case. However, the most important part is the application of materials. Making passing paths for CO_2 is a good concept, however, an investigation from the perspective of materials should be the first priority. Comprehensively, the key component for capturing CO_2 was CaO [6]. In addition, all existing studies only used the materials themselves, without any special treatment. In addition, those materials contained reactive components, therefore, the loss of materials occurred through reactions during cement hydration [4,13,14]. The purpose of CO_2 capturing is to accelerate the reaction and maximize the sequestration efficiency. In order to achieve these conditions, it is important that the CO_2 reactant survives in an unreacted state. Therefore, a study on this aspect should be carried out.

The investigation of CO_2 movement paths was carried out by artificially increasing the internal spaces, but in no case was a general hardened cement paste product used.

In addition, there were few cases in which additional methods for protecting reactants were considered. Therefore, it was judged that it is necessary to investigate the effect of the CO_2 path through a general hardened cement paste product in a general state, and to study improvement in CO_2 sequencing performance through the coating protection of CH granules. This study focused on using CH as a CO_2 reactant and maximizing CO_2 capturing performance, while preventing this material from reacting with cement as much as possible using granulation and coating techniques. Through this technique, it was expected that the CO_2 sequestration performance of cement composites would be increased remarkably.

2. Materials and Experiments

2.1. Materials

The binder was the ordinary Portland cement (OPC), defined in the ASTM C150 [15]. The OPC which was used in this study is a type I cement whose composition can be easily found in other studies, and is listed in Table 1 [16–18].

Table 1. Properties of OPC.

Chemical Composition (%)					
SiO_2	**Al_2O_3**	**Fe_2O_3**	**CaO**	**MgO**	**Other**
20.8	6.3	3.2	62	3.3	4.4
Physical Properties					
Blaine (cm^2/g)			**Specific Gravity (ton/m^3)**		
3200			3.15		

Natural sand was used as the fine aggregate, with a fineness modulus of 2.55, a density of 2.63 ton/m^3, a water absorption of 1.35%, and particle size distribution (PSD) as shown in Figure 1 [19].

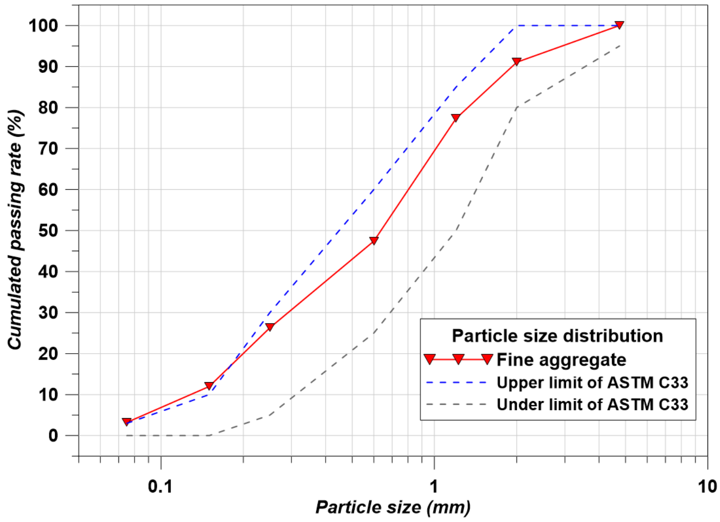

Figure 1. PSDs of fine aggregate.

In this study, to accelerate CO_2 capturing, CH was used as a granule material. Because CO_2 reacts with the calcium in the cement matrix [20], the CH was considered the most suitable material for CO_2 capturing. To granulate the CH, a binder was needed to bond the CH particles, and the material chosen was hydroxypropyl methylcellulose (HPMC), HPMC 2910. In addition, to prevent the reaction between the OPC and granulated CH, a coating process was added, and the coating material was a hydrophilic material, HPMC 2208. Since the coating should be molten in order for the granulated CH to react with CO_2, HPMC 2208 was a suitable choice for the coating material. Here, HPMC numbers (2910 and 2208) refer to the grade of HPMC. Its details are indicated in Table 2, and the method of this study is presented in Figure 2.

Table 2. Details of the granulation materials.

Type	Details of Materials
Granule	• Main composition: CH (95%) • Diameter: 0.3 mm, Length: 0.4~0.6 mm
Granule binder	• Main composition: HPMC with grade 2910 (HPMC 2910) • Viscosity: 3 mPa·s • HPMC-to-solvent ratio: 1%
Coating material	• Main composition: HPMC with grade 2208 (HPMC 2208) • Viscosity: 100,000 mPa·s • HPMC-to-solvent ratio: 0.25% • Coating method: rotating pan coating
Solvent	• 5 M of NaOH solution

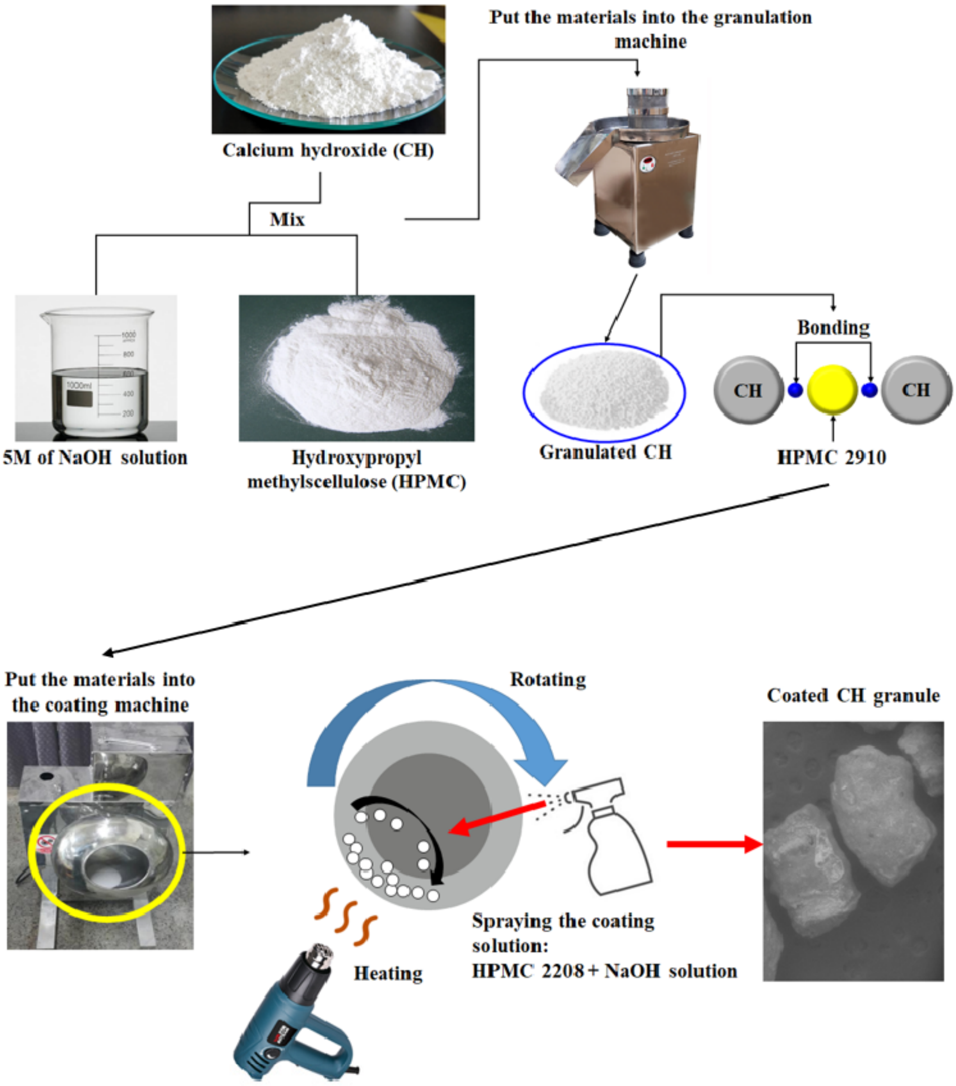

Figure 2. The process of making the coated CH granules.

The coated CH granules (CCHG), as shown in Figure 3, were used as an additive material, and the dosage ratio was 5% of the cement weight. The reason for the 5% dosage was that the HPMC is an organic material, and organic material usually decreases the mechanical performance of cement composites [21–23]. Because of this negative effect, the dosage of organic additive had to be less than 5% of the cement weight [22] or water weight [21]. Therefore, a dosage ratio of 5% of the cement weight was chosen, considering both strength performance and CO_2 sequestration performance. The mix's details are presented in Table 3.

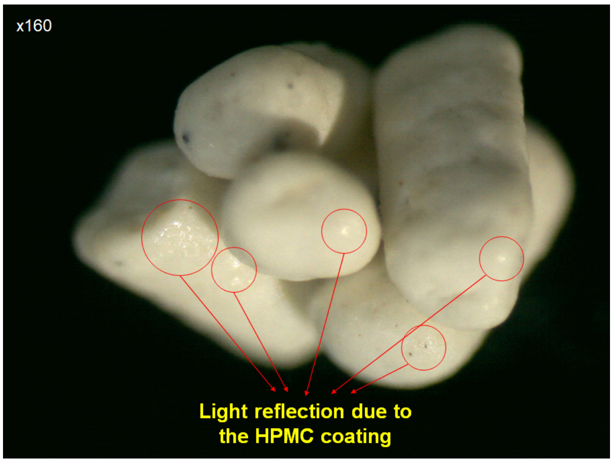

(**a**) Before CO_2-ppm.

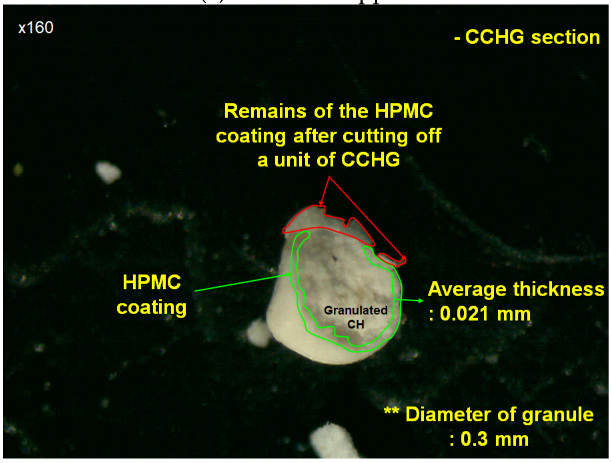

(**b**) After CO_2-ppm.

Figure 3. Coated CH granules.

Table 3. Mix details.

Specimens	Mix Ratio (On the Basis of Cement)					
	Water	Cement	Sand	CCHG	Fly Ash	BFS [1]
C-G0	0.485	1	2.75	0	0	0
F-G0					0.1	0
S-G0					0	0.1
C-G5				0.05	0	0
F-G5					0.1	0
S-G5					0	0.1

[1] BFS = blast furnace slag.

Additionally, commonly used by-products, which were fly ash (FA) and blast furnace slag (BFS), were used. It is already well known that FA and BFS improve the durability of cement composites [24,25]. Because the pozzolanic components cause the pozzolan effect [26,27] and the particle size of FA and BFS causes the packing effect [28], most of the performance factors of the cement composites (including durability) improve.

BFS has sufficient potential for the sequestration of CO_2 [29,30], since BFS has a sufficient amount of CaO, as shown in Table 4. In addition, the CO_2-capturing performance of the FA shows that FA also has enough potential for the sequestration of CO_2 [31], the composition of FA is shown in Table 4.

Table 4. Chemical composition of FA and BFS.

Materials	SiO_2	Al_2O_3	Fe_2O_3	CaO	LOI
FA	56.4	23.2	7.6	3.3	1.0
BFS	34.5	16.1	0.6	42.6	0.05

2.2. Experiment

To investigate the CO_2 sequestration performance, CO_2 sequestration monitoring was carried out by ppm (CO_2-ppm), X-ray diffraction (XRD), mercury intrusion porosimetry (MIP), and Fourier transform infra-red (FTIR). All the specimens were cured for 91 days in the air, with 65% relative humidity and 20 °C air temperature. The reason for the long duration of curing was that we intended to wait for the coated material to undergo a full phase-change. Due to the long duration of curing, components such as ettringite disappeared, and only core components like CSH, portlandite, and calcite remained. Therefore, the analysis was simplified due to the long-term curing. The comprehensive process of the experiment is presented in Figure 4.

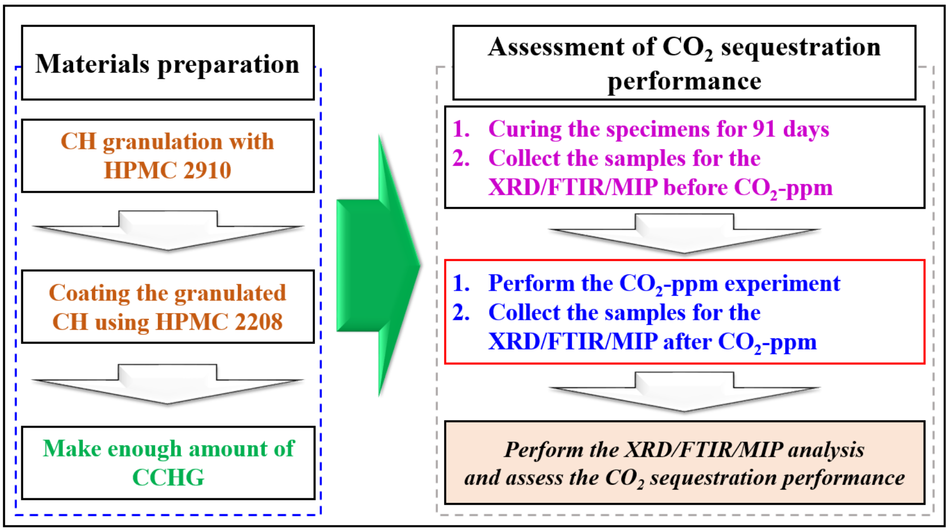

Figure 4. Comprehensive process of the experiment.

2.2.1. CO_2 Sequestration Monitoring by ppm (CO_2-ppm)

To specifically assess the CO_2 sequestration performance, some factors were controlled. The concentration of CO_2 was controlled at 99.99% in the atmosphere because the concentration of CO_2 in the air is quite low. The CO_2 concentration controlling system is indicated in Figure 5. To bring the concentration of CO_2 to 100% in the desiccator, the inside of desiccator featured a specifically made vacuum. After vacuuming the inside of the desiccator, the air flowing pipe at the side linked with the vacuum pump was closed, and the pipe at the side linked with the CO_2 tank was opened. The inside of the desiccator was completely filled with CO_2 from the CO_2 tank, and the injection status of CO_2 was monitored using the air pressure gauge installed in the desiccator. In addition, the CO_2 concentration was checked using the CO_2 sensor (Econarae Co., Yongin-Si, Republic of Korea, Accuarcy—99% ± 0.5%) installed in the desiccator. While the CO_2 reacts with CCHG, water is generated, and the generated water makes the sensing accuracy decrease, because the CO_2 sensor is sensitive to humidity. Thus, a super absorbent polymer (SAP) was placed in the desiccator to absorb the generated water. Including the CO_2 controlling system, the full experimental system is shown in Figure 6.

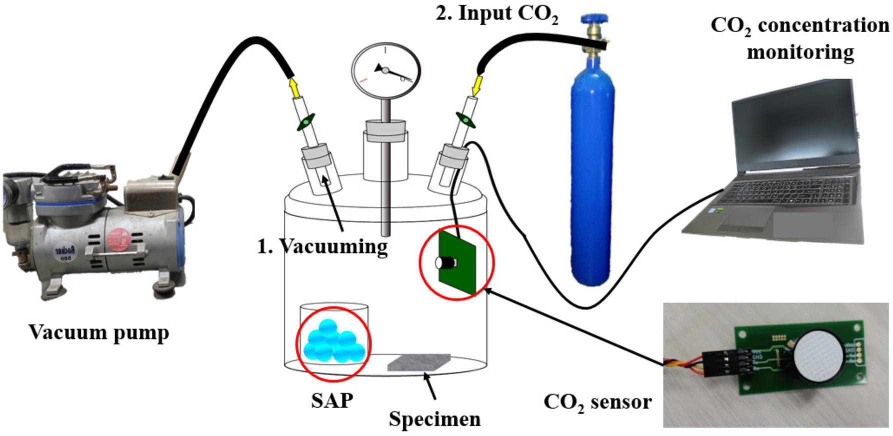

Figure 5. CO_2 concentration control.

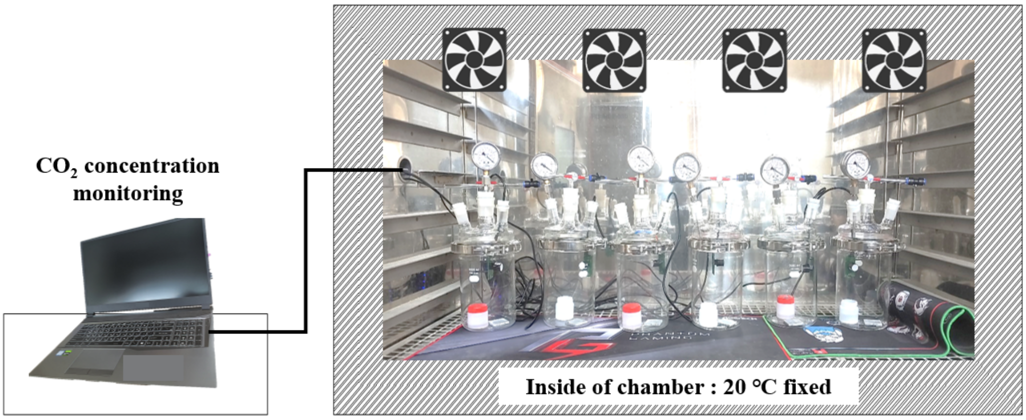

Figure 6. CO_2 sequestration experiment.

Cement composites are a kind of heterogeneous material. Thus, their temperature should be fixed, because fine aggregate and CCHG particles are randomly placed in the cement matrix. Randomly placed materials can not be controlled, therefore, it is essential to fix the outside temperature. The desiccators containing the specimens were placed in the temperature-controlled chamber, and the room temperature of the chamber was fixed to 20 °C for a measuring duration of 5 days.

2.2.2. X-ray Diffraction (XRD)

The reaction between CCHG and CO_2 was confirmed by crystallization, and the results were confirmed by the XRD. The XRD specifics were 40 kV, 3 mA, a scanning speed of 2°/min, and a wavelength of 1.54 Å (D/max2500, Rigaku Corporation, Tokyo, Japan). All the specimens' crystalline components were measured by XRD before CO_2-ppm and after CO_2-ppm. Through these comparisons, the reaction of CCHG could be confirmed.

2.2.3. Fourier Transform Infra-Red (FTIR)

The crystalline production could be confirmed by XRD, however, we could not sufficiently demonstrate the sequestration performance with only XRD. For the exact evaluation of CO_2 sequestration performance, supporting analyses were needed, and FTIR (Nicolet 6700, Thermo Scientific, Waltham, MA, USA) was one of them. Through the FTIR, the reaction details between CO_2 and CCHG were analyzed.

2.2.4. Mercury Intrusion Porosimetry (MIP)

The distinctive characteristic of this study was that the matrix of specimens was denser than before the CO_2-ppm experiment. However, this general assumption could have been made before the experiment was carried out, therefore, we needed to demonstrate how much the porosity decreased. In the MIP test (Micromeritics Autopore IV 9500, Micromeritics Instrument Co., Norcross, GA, USA), the pore size could be calculated by Equation (2):

$$\gamma = \frac{-2\delta cos\theta}{p} \tag{2}$$

where γ is the radius of pore (µm), δ is the mercury surface tension (N/m, with 0.484 N/m applied), θ is the contact angle between the specimen and mercury (with 130° applied), and p is the input pressure of mercury (with 206.84 MPa applied). Following the pressure, the measurable pore size was 3 nm.

2.2.5. Thermogravimetric Analysis (TGA)

CO_2-ppm was the intuitive method chosen for showing that the CO_2 sequestration performance, and TGA (TGA7 PERKIN ELMER, TA Instruments, New Castle, DE, USA) was the quantitative method chosen for showing that the trend of the chemical analysis was right. The temperature range was 25 to 900 °C. CH and CC were mainly checked, and in particular, the increments in CC before and after the CO_2-ppm experiment.

3. Results and Discussion

3.1. CO_2-ppm Results with MIP

The CO_2-ppm trends were clear. S-G0 and S-G5 were expected to show the best performance in CO_2 sequestration due to their CaO contents with BFS and cement. However, according to Figure 7, it was unexpected that the C-G0 and C-G5 would show the best sequestration performance.

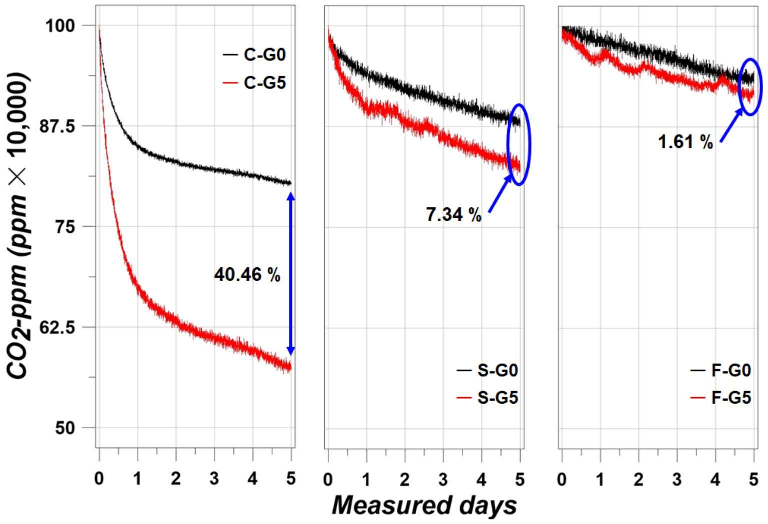

Figure 7. CO_2-ppm results.

There was a large gap in the absorbed amount of CO_2 compared to C-G0, C-G5, and the other specimens. In the case of C-G5, the absorbed amount of CO_2 was increased to 40.46% compared to C-G0. C-G0 absorbed the CO_2 at about 198,000 ppm, and C-G5 absorbed the CO_2 at about 429,000 ppm. This was evidence that the CCHG significantly improved the CO_2 sequestration. However, the other specimens showed a relatively poor sequestration performance compared with C-G0 and C-G5. It was considered that the filler effect from BFS and FA disturbed the improvement in CO_2 sequestration performance. As is well known, BFS and FA make cement composites denser [32,33]. This means that the porosity is reduced, in other words, the path of airflow is also reduced. This concept can be explained roughly by Figure 8.

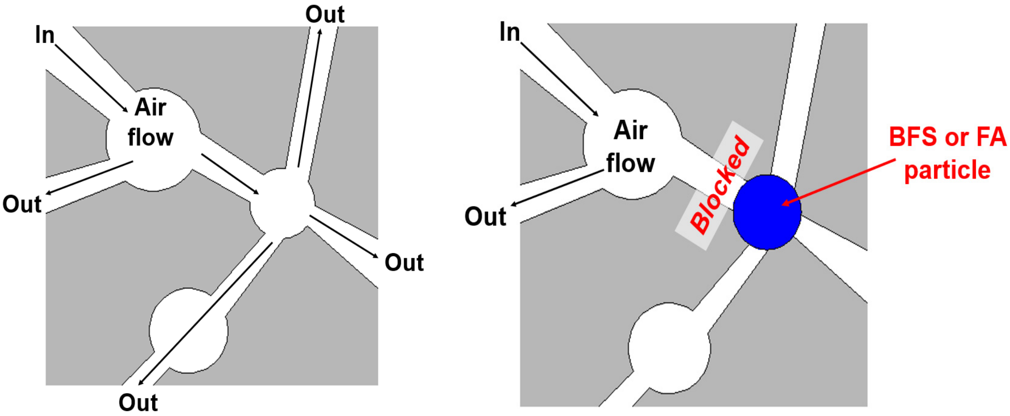

(**a**) Normal air path. (**b**) Air path blocked by BFS or FA.

Figure 8. The case of normal and blocked air paths in the cement matrix.

The concept of Figure 8 is directly related to air permeability, and it has been reported that BFS and FA reduce air permeability significantly [34]. When the air path was blocked by BFS or FA particles, the CO_2 flow was also significantly disturbed. Evidence for the concept of Figure 8 is in the porosity trends shown in Figure 9.

Like the trends reported in [32–34], the porosity results showed that S g series and F g series showed less porosity than C g series. In addition, CCHG also brought about a minimal filler effect, as confirmed by Figure 9. Overall, the reason that the CO_2-ppm results appeared as in Figure 7 can be understood using Figures 8 and 9.

The S g and F g series showed a strong packing phenomenon, as shown in Figure 9. Within this phenomenon, it was considered that the blocking of air flow in the cement matrix was reduced significantly by the BFS and FA particles. Most studies on the carbonation of cement composites have focused on preventing or reducing carbonation depth [35]. Therefore, the results in Figure 9 are commonly understood. However, interestingly, the use of BFS or FA brought about a negative effect on absorbing CO_2 in this study. Due to the packing effect shown in Figure 8, CO_2 could not flow in the cement matrix, therefore, CO_2 could not touch the CCHG. Then, the CCHG could not sequestrate the CO_2, and the CO_2-ppm efficiency was significantly decreased by the packing effect.

Paradoxically, contrary to what is well-known, the use of BFS and FA led to a decrease in CO_2 sequestration performance by reducing the porosity and blocking the path of CO_2. Here, a new factor was found: a higher porosity had a good effect on improving the CO_2 sequestration performance of the cement composites.

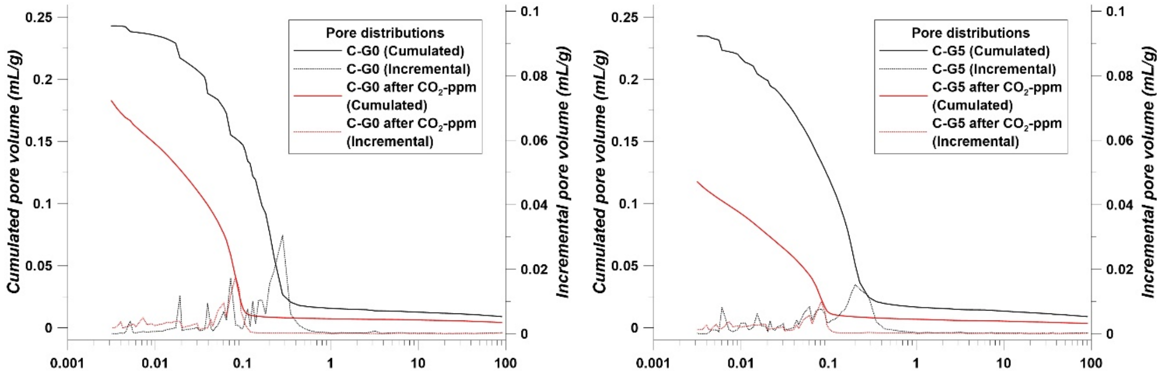

(**a**) MIP result of C-G0. (**b**) MIP result of C-G5.

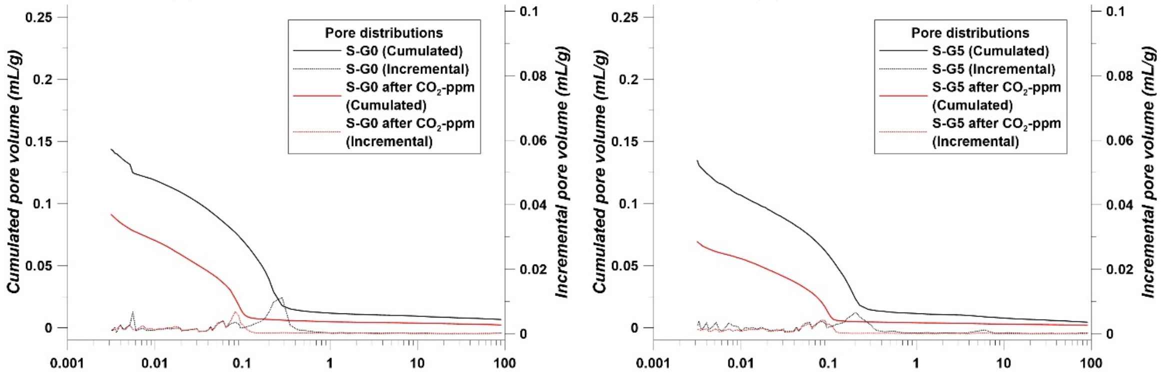

(**c**) MIP result of S-G0. (**d**) MIP result of S-G5.

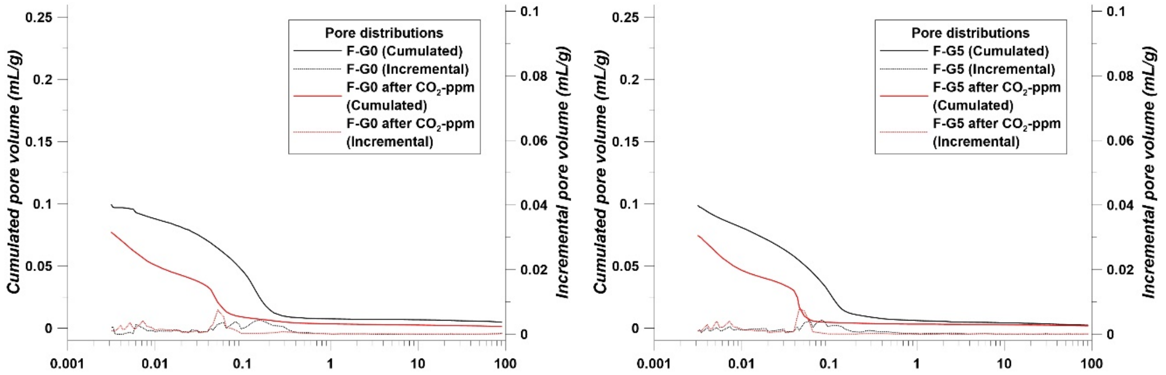

(**e**) MIP result of F-G0. (**f**) MIP result of F-G5.

Figure 9. MIP results.

3.2. XRD Resutls

According to the XRD data in Figure 10, calcite was detected in all the cases after CO_2-ppm. The theta degrees of 17.98, 34.10, 47.12, 50.81 indicate portlandite, and it can be confirmed that portlandite clearly disappeared, especially at the theta degree of 17.98 in the G0 case. These results indicate that carbonation proceeded normally [36]. However, an interesting point was that portlandite was detected in all the G5 specimens after CO_2-ppm at the theta degree of 47.12 and 50.81. This phenomenon appeared when the portlandite remained after carbonation, in this case, the intensity at the theta degree of 17.98 was very weakly detected, or not detected at all [37]. However, at theta degrees of 47.12 and 50.81, the remaining portlandite could be detected [37]. Therefore, portlandite points were detected after CO_2-ppm in the cases of G5 specimens.

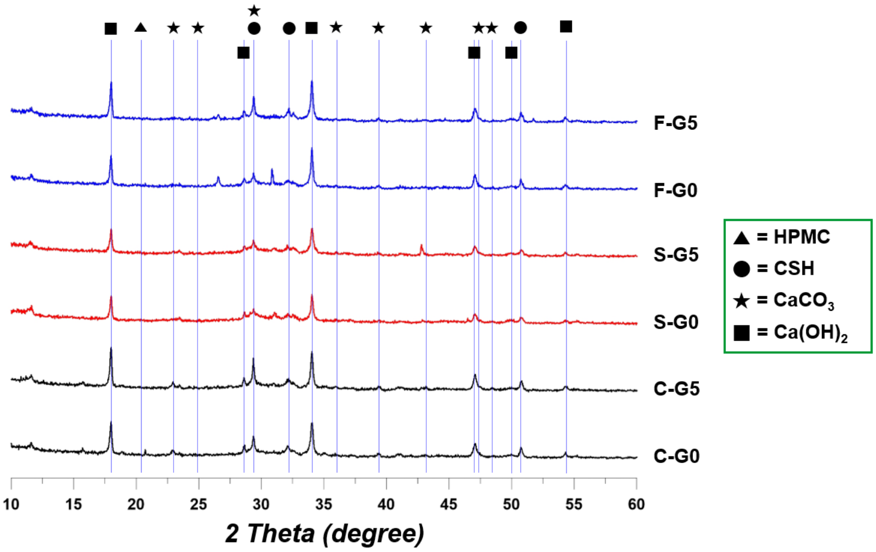

(**a**) Before CO_2-ppm.

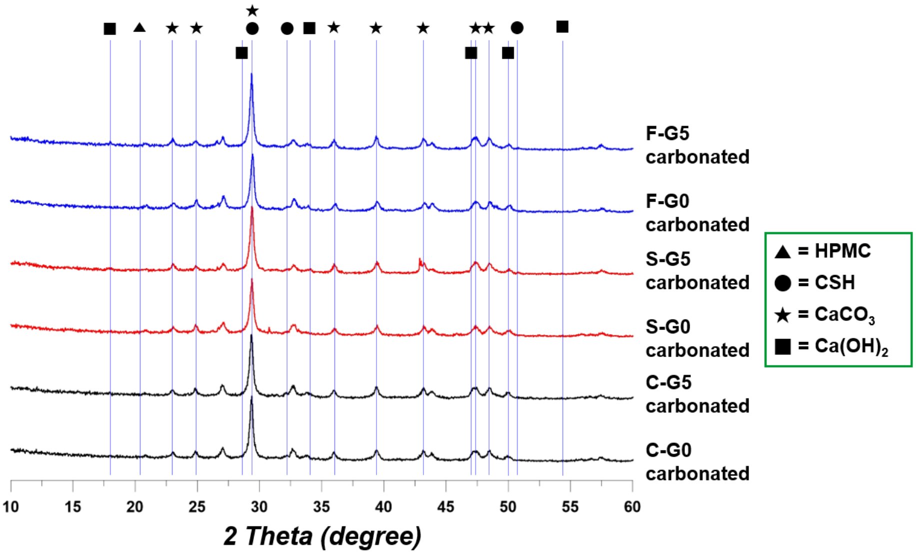

(**b**) After CO_2-ppm.

Figure 10. XRD results.

From the XRD results, it was demonstrated that the CCHG absorbed the CO_2 enough, and the CCHG produced calcite after reacting with CO_2. In addition, the HPMC fully disappeared due to the long-term curing.

3.3. FTIR Results

The FTIR results showed a remarkable difference between before and after CO_2-ppm. The most distinctive difference was the calcite. As in the XRD results, the wavelength absorption was significantly increased at the calcite points in all specimens. The FTIR results are indicated in Figure 11.

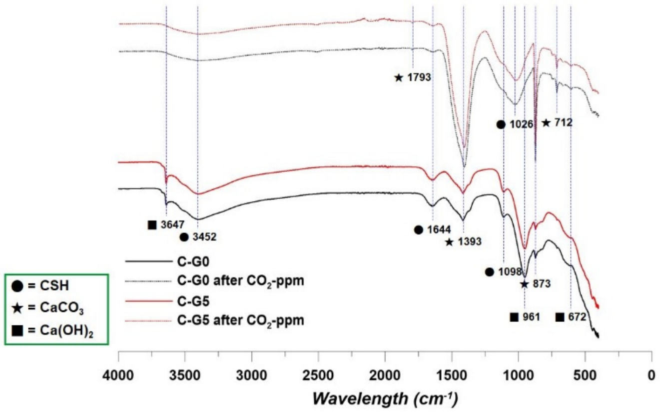

(**a**) FTIR results of C-G0 and C-G5.

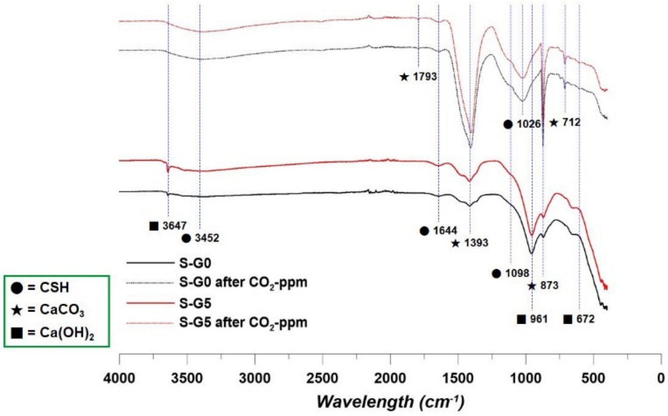

(**b**) FTIR results of S-G0 and S-G5.

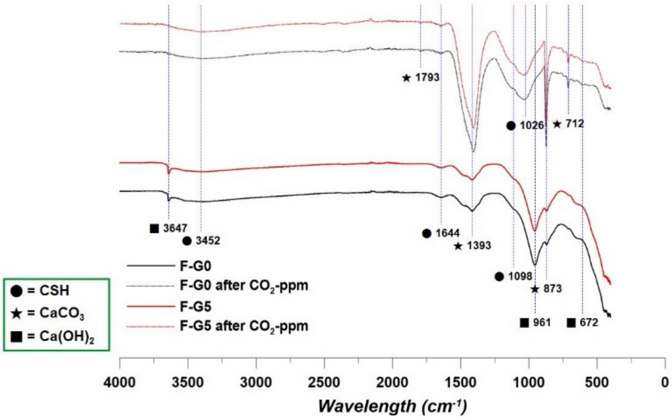

(**c**) FTIR results of F-G0 and F-G5.

Figure 11. FTIR results.

Due to the long-term curing, the portlandite intensities were different. The curing duration was enough time for the pozzolanic reaction. Therefore, the intensity points of portlandite in the F g and S g series were relatively more weakly detected than in the C g series [38]. At the characteristic 3452 wavelength point in the cases of F g and S g specimens, the intensity was increased after CO_2-ppm, because the BFS and FA consumed the CH, and it made the CSH [38]. In addition, all the cases showed the intensity of CSH was weakened, not indicating a reduction in CSH, but instead indicating an increase in calcite.

All the data from CO_2-ppm, MIP, XRD, and FTIR indicated an increase in calcite after the reaction of CCHG and CO_2. In addition, due to the pozzolanic reaction, CH was consumed, and this led to a reduction in the CO_2 sequestration performance, because CH was the key component in consuming CO_2.

3.4. TGA Results

TGA results are presented in Figure 12. The distinct difference was the detected absolute amount of CC. Usually, the CH appears around 420 °C, and the CC appears in the range of 550 to 740 °C [39,40]. The amount of CC before/after CO_2-ppm showed the same trend as the XRD and FTIR results. The intensity of the CH disappeared after CO_2-ppm according to the XRD and FTIR, but the intensity of CC increased in all cases. Showing the same trend, the amount of CC increased in the TGA data after the CO_2-ppm. Compared to the MIP results, the absolute amount of CC after CO_2-ppm proved that the pores in the cement matrix were important to sequestrate the CO_2. Due to the filler effect, as mentioned in the MIP chapter, the moving path of CO_2 was blocked or narrowed by the FA and BFS. Therefore, the increment in and absolute amount of CC tended to decrease after CO_2-ppm, as shown in Figure 12. In addition, the CH peaks almost disappeared in all specimens after CO_2-ppm, this meant that the peaks in XRD and FTIR showed the components accurately.

3.5. Summary Discussion

The performance improvement in CO_2 sequestration with CCHG was demonstrated by the CO_2-ppm. In addition, it was focused on obtaining the reliability of CO_2 sequestration performance through a component analysis by XRD and FTIR, and porosity confirmation by MIP. Before carrying out the CO_2-ppm, the problem was that the coated HPMC was fully phase-changed. This point was confirmed by the XRD patterns. The peak of HPMC appeared nearby the theta degree of 20 [41], and the peak of HPMC was not detected in all the cases of G5 specimens. Therefore, it can be considered that the coated HPMC was fully phase-changed.

The CO_2-ppm experiment results were unexpected, because existing studies have reported that the BFS and FA are helpful to sequestrate the CO_2 [42,43]. Of course, those existing studies treated the materials to meet the aim of their studies. However, the usual cases use the FA or BFS as a supplementary material to the cement, therefore, the packing effect of FA and BFS [32–34] had a negative effect on the CO_2 sequestration in this study. The packing effect was confirmed by the MIP results, which showed that the porosity was significantly reduced than C-G0 and C-G5 before CO_2-ppm. In addition, the pozzolanic reaction was also confirmed due to the long-term curing. The pozzolan reaction consumes the CH to make the CSH, therefore, the amount of CH was reduced in the cases of F g and S g specimens, and it led to the reduction of CO_2 sequestration performance.

Comprehensively, to sequestrate the CO_2 enough, higher porosity was helpful in capturing the $CO_{2,}$ paradoxically. This is because the packing effect caused the blocking of the path of air flow, and it disturbed the reaction between CCHG and CO_2. However, high porosity caused a reduction in the mechanical strength [44]. Therefore, the concept of this study should not be applied to main structures such as columns, slabs, and beams, because this concept needs high porosity, and thus may not have enough strength. Thus, this concept is suitable for substructures that are not burdened by external loads, such as the median strip on roads.

One limitation of this study is the use of a lot of CH powders to make granules. The procedure for making CH powders needs high temperatures, like the production of cement. High production temperature definitely produces CO_2. Hence, further works should use other materials that have high reactivity with CO_2 and low production temperatures with the method of this study to overcome this limitation.

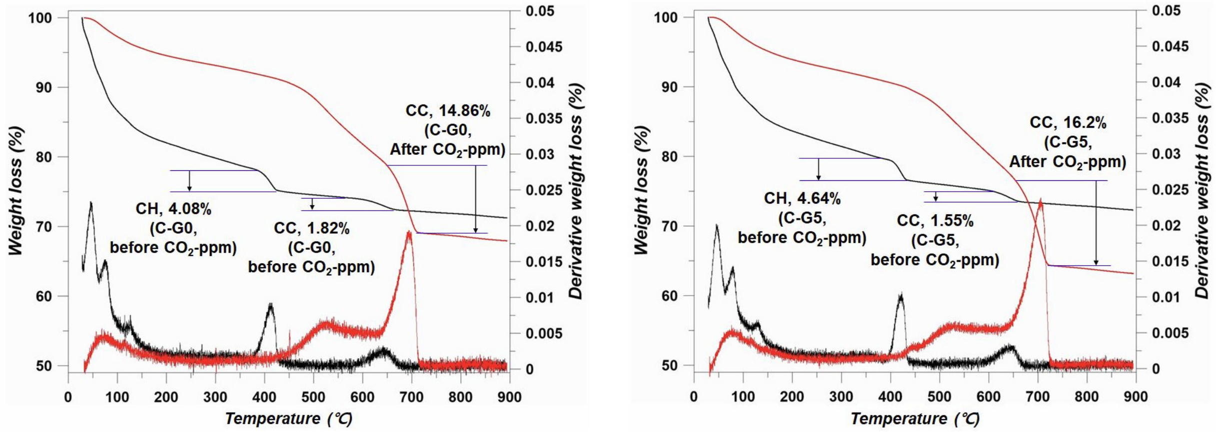

(**a**) TGA result of C-G0. (**b**) TGA result of C-G5.

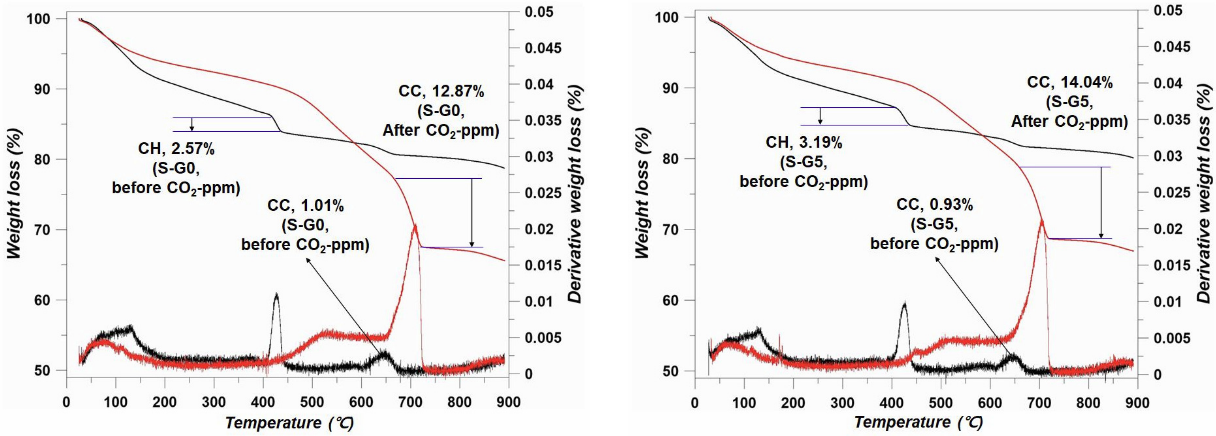

(**c**) TGA result of S-G0. (**d**) TGA result of S-G5.

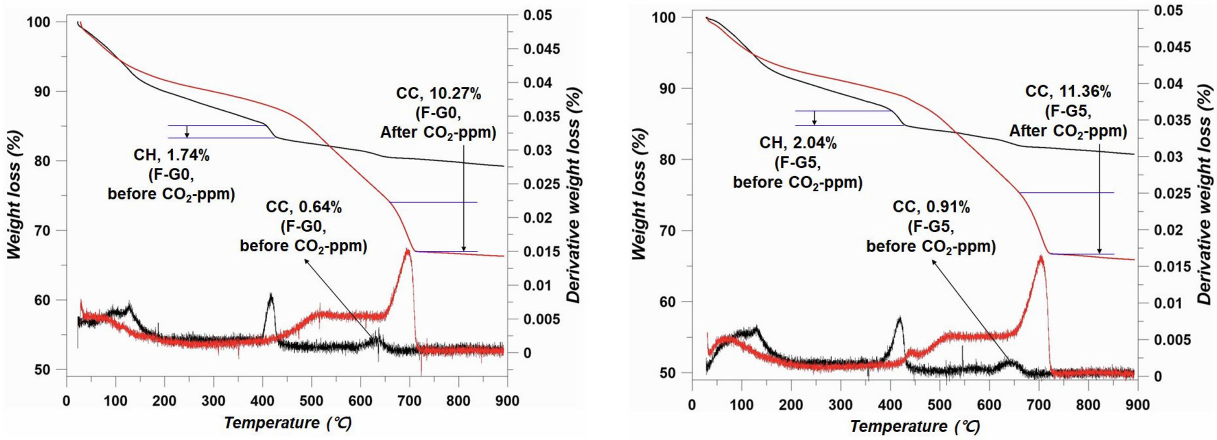

(**e**) TGA result of F-G0. (**f**) TGA result of F-G5.

Figure 12. TGA results.

4. Conclusions

This study focused on improving the CO_2 sequestration performance of cement composites using a granulation technique. The main material was CH, and the binder of CH was HPMC 2910. The granulated CH should not be in the reactive state, therefore, it needed a coating to prevent the reaction between cement paste and granulated CH while the cement composites were curing. The granules were coated with HPMC 2208 and the specimens with CCHG were cured for 91 days to wait for the coating to fully phase-change. Our comprehensive conclusions are as follows:

1. The CO_2-ppm results were contrary to the expectation that the F g and S g groups would show better performance than the C g group. This is because the BFS and FA caused the filler effect, and this phenomenon blocked the path of CO_2 flow as result. Therefore, CCHG could not react with CO_2 enough because of the BFS and FA. In short, BFS and FA had a negative effect on the CO_2 sequestration performance.
2. According to the XRD, FTIR, and TGA results, one other negative factor was found: the pozzolan effect caused the consumption of CH. As is well known, the pozzolan reaction consumes CH to make CSH. However, CH is a key component in reacting with CO_2 in the cement matrix, therefore, the amount of CH was decreased by the pozzolan reaction during the curing period. The CH consumption was found in the results of XRD, FTIR, and TGA. Due to this phenomenon, combined with the filler effect, the sequestration performance was significantly decreased.
3. As a comprehensive result, CO_2 sequestration depends on the porosity and the amount of CH in the cement matrix. For this reason, the matrix did not have enough strength, therefore, the concept of this study is suitable for substructures are not burdened by external loads, such as the median strip on roads.

Author Contributions: J.-B.L. Methodology, Resources, Funding acquisition; J.-H.K. Conceptualization, Validation, Formal analysis, Investigation; B.-G.M. Supervision, Project administration, Validation, Formal analysis; B.-H.W. Conceptualization, Writing—original draft, Writing—review and editing, Supervision. All authors have read and agreed to the published version of the manuscript.

Funding: This research was supported by a Korea Agency for Infrastructure Technology Advancement (KAIA) grant funded by the Korean government (MOLIT) (RS-2023-00250434).

Institutional Review Board Statement: Not applicable.

Informed Consent Statement: Not applicable.

Data Availability Statement: Data are contained within the article.

Conflicts of Interest: The authors declare no conflict of interest.

References

1. Costa, F.N.; Ribeiro, D.V. Reduction in CO_2 Emissions during Production of Cement, with Partial Replacement of Traditional Raw Materials by Civil Construction Waste (CCW). *J. Clean. Prod.* **2020**, *276*, 123302. [CrossRef]
2. Sanjuán, M.Á.; Andrade, C.; Mora, P.; Zaragoza, A. Carbon Dioxide Uptake by Mortars and Concretes Made with Portuguese Cements. *Appl. Sci.* **2020**, *10*, 646. [CrossRef]
3. Nie, S.; Zhou, J.; Yang, F.; Lan, M.; Li, J.; Zhang, Z.; Chen, Z.; Xu, M.; Li, H.; Sanjayan, J.G. Analysis of Theoretical Carbon Dioxide Emissions from Cement Production: Methodology and Application. *J. Clean. Prod.* **2022**, *334*, 130270. [CrossRef]
4. Skocek, J.; Zajac, M.; Ben Haha, M. Carbon Capture and Utilization by Mineralization of Cement Pastes Derived from Recycled Concrete. *Sci. Rep.* **2020**, *10*, 5614. [CrossRef]
5. Huntzinger, D.N.; Gierke, J.S.; Sutter, L.L.; Kawatra, S.K.; Eisele, T.C. Mineral Carbonation for Carbon Sequestration in Cement Kiln Dust from Waste Piles. *J. Hazard. Mater.* **2009**, *168*, 31–37. [CrossRef]
6. Bobicki, E.R.; Liu, Q.; Xu, Z.; Zeng, H. Carbon Capture and Storage Using Alkaline Industrial Wastes. *Prog. Energy Combust. Sci.* **2012**, *38*, 302–320. [CrossRef]
7. Eloneva, S.; Teir, S.; Salminen, J.; Fogelholm, C.J.; Zevenhoven, R. Fixation of CO_2 by Carbonating Calcium Derived from Blast Furnace Slag. *Energy* **2008**, *33*, 1461–1467. [CrossRef]
8. Roy, P.; Mohanty, A.K.; Wagner, A.; Sharif, S.; Khalil, H.; Misra, M. Impacts of COVID-19 Outbreak on the Municipal Solid Waste Management: Now and beyond the Pandemic. *ACS Environ. Au* **2021**, *1*, 32–45. [CrossRef]
9. Woo, B.H.; Jeon, I.K.; Yoo, D.H.; Kim, S.S.; Lee, J.B.; Kim, H.G. Utilization of Municipal Solid Waste Incineration Bottom Ash as Fine Aggregate of Cement Mortars. *Sustainability* **2021**, *13*, 8832. [CrossRef]
10. Rendek, E.; Ducom, G.; Germain, P. Carbon Dioxide Sequestration in Municipal Solid Waste Incinerator (MSWI) Bottom Ash. *J. Hazard. Mater.* **2006**, *128*, 73–79. [CrossRef]
11. Luo, W.; Li, B.; Xu, M.; Pang, C.; Lester, E.; Xu, L.; Kow, K.W. In-Situ Release and Sequestration of CO_2 in Cement Composites Using LTA Zeolites. *Sci. Total Environ.* **2023**, *872*, 162133. [CrossRef]
12. Gupta, S.; Kashani, A.; Mahmood, A.H. Carbon Sequestration in Engineered Lightweight Foamed Mortar–Effect on Rheology, Mechanical and Durability Properties. *Constr. Build. Mater.* **2022**, *322*, 126383. [CrossRef]
13. Kang, S.; Kang, H.; Lee, B. Effects of Adding Neutralized Red Mud on the Hydration Properties of Cement Paste. *Materials* **2020**, *13*, 4107. [CrossRef]

14. Zhang, S.; Ghouleh, Z.; He, Z.; Hu, L.; Shao, Y. Use of Municipal Solid Waste Incineration Bottom Ash as a Supplementary Cementitious Material in Dry-Cast Concrete. *Constr. Build. Mater.* **2021**, *266*, 120890. [CrossRef]
15. *ASTM C150*; Standard Specification for Portland Cement. ASTM International: West Conshohocken, PA, USA, 2017.
16. Aodkeng, S.; Sinthupinyo, S.; Chamnankid, B.; Hanpongpun, W.; Chaipanich, A. Effect of Carbon Nanotubes/Clay Hybrid Composite on Mechanical Properties, Hydration Heat and Thermal Analysis of Cement-Based Materials. *Constr. Build. Mater.* **2022**, *320*, 126212. [CrossRef]
17. Pei, J.; Sharma, R.; Jang, J.G. Use of Carbonated Portland Cement Clinkers as a Reactive or Non-Reactive Aggregate for the Production of Cement Mortar. *Constr. Build. Mater.* **2022**, *319*, 126070. [CrossRef]
18. Wang, F.; Li, K.; Liu, Y. Optimal Water-Cement Ratio of Cement-Stabilized Soil. *Constr. Build. Mater.* **2022**, *320*, 126211. [CrossRef]
19. *ASTM C33*; Standard Specifications for Concrete Aggregates. ASTM International: West Conshohocken, PA, USA, 2003.
20. You, X.; Hu, X.; He, P.; Liu, J.; Shi, C. A Review on the Modelling of Carbonation of Hardened and Fresh Cement-Based Materials. *Cem. Concr. Compos.* **2022**, *125*, 104315. [CrossRef]
21. Aquilina, A.; Borg, R.P.; Buhagiar, J. The Application of Natural Organic Additives in Concrete: Opuntia Ficus-Indica. In Proceedings of the IOP Conference Series: Materials Science and Engineering, Valletta, Malta, 10 April 2018; Institute of Physics Publishing: Bristol, UK, 2018; Volume 442.
22. Kamorny, D.A.; Safonov, A.V.; Boldyrev, K.A.; Abramova, E.S.; Tyupina, E.A.; Gorbunova, O.A. Modification of the Cement Matrix with Organic Additives for Stabilizing Pertechnetate Ions. *J. Nucl. Mater.* **2021**, *557*, 153295. [CrossRef]
23. Patel, G.K.; Deo, S.V. Effect of Natural Organic Materials as Admixture on Properties of Concrete. *Indian. J. Sci. Technol.* **2016**, *9*, 1–8. [CrossRef]
24. Humad, A.M.; Kothari, A.; Provis, J.L.; Cwirzen, A. The Effect of Blast Furnace Slag/Fly Ash Ratio on Setting, Strength, and Shrinkage of Alkali-Activated Pastes and Concretes. *Front. Mater.* **2019**, *6*, 9. [CrossRef]
25. Teixeira, E.R.; Camões, A.; Branco, F.G. Synergetic Effect of Biomass Fly Ash on Improvement of High-Volume Coal Fly Ash Concrete Properties. *Constr. Build. Mater.* **2022**, *314*, 125680. [CrossRef]
26. Bui, P.T.; Ogawa, Y.; Kawai, K. Long-Term Pozzolanic Reaction of Fly Ash in Hardened Cement-Based Paste Internally Activated by Natural Injection of Saturated $Ca(OH)_2$ Solution. *Mater. Struct. Mater. Et. Constr.* **2018**, *51*, 144. [CrossRef]
27. Ustabaş, İ.; Kaya, A. Comparing the Pozzolanic Activity Properties of Obsidian to Those of Fly Ash and Blast Furnace Slag. *Constr. Build. Mater.* **2018**, *164*, 297–307. [CrossRef]
28. Liu, X.; Yu, R.J. Blast Furnace Slag Foundation Packing Grading and Compaction Characteristics Analysis. *Appl. Mech. Mater.* **2013**, *368*, 855–859. [CrossRef]
29. Jeon, I.K.; Kim, H.G.; Jakhrani, S.H.; Ryou, J.S. Evaluation of the Microstructure, Mechanical, and Durability Properties of Alkali-Activated Slag-Based Mortar with Light-Burnt Dolomite Powder. *J. Mater. Res. Technol.* **2021**, *13*, 2220–2228. [CrossRef]
30. Yasipourtehrani, S.; Tian, S.; Strezov, V.; Kan, T.; Evans, T. Development of Robust CaO-Based Sorbents from Blast Furnace Slag for Calcium Looping CO_2 Capture. *Chem. Eng. J.* **2020**, *387*, 124140. [CrossRef]
31. Dindi, A.; Quang, D.V.; Vega, L.F.; Nashef, E.; Abu-Zahra, M.R.M. Applications of Fly Ash for CO_2 Capture, Utilization, and Storage. *J. CO2 Util.* **2019**, *29*, 82–102. [CrossRef]
32. Hsu, S.; Chi, M.; Huang, R. Effect of Fineness and Replacement Ratio of Ground Fly Ash on Properties of Blended Cement Mortar. *Constr. Build. Mater.* **2018**, *176*, 250–258. [CrossRef]
33. Kim, J.; Na, S.; Hama, Y. Effect of Blast-Furnace Slag Replacement Ratio and Curing Method on Pore Structure Change after Carbonation on Cement Paste. *Materials* **2020**, *13*, 4787. [CrossRef]
34. Katpady, D.N.; Hazehara, H.; Soeda, M.; Kubota, T.; Murakami, S. Durability Assessment of Blended Concrete by Air Permeability. *Int. J. Concr. Struct. Mater.* **2018**, *12*, 30. [CrossRef]
35. Gruyaert, E.; Van Den Heede, P.; De Belie, N. Carbonation of Slag Concrete: Effect of the Cement Replacement Level and Curing on the Carbonation Coefficient-Effect of Carbonation on the Pore Structure. *Cem. Concr. Compos.* **2013**, *35*, 39–48. [CrossRef]
36. Song, K.I.; Song, J.K.; Lee, B.Y.; Yang, K.H. Carbonation Characteristics of Alkali-Activated Blast-Furnace Slag Mortar. *Adv. Mater. Sci. Eng.* **2014**, *2014*, 326458. [CrossRef]
37. Vance, K.; Falzone, G.; Pignatelli, I.; Bauchy, M.; Balonis, M.; Sant, G. Direct Carbonation of $Ca(OH)_2$ Using Liquid and Supercritical CO_2: Implications for Carbon-Neutral Cementation. *Ind. Eng. Chem. Res.* **2015**, *54*, 8908–8918. [CrossRef]
38. Ashish, D.K.; Verma, S.K. Cementing Efficiency of Flash and Rotary-Calcined Metakaolin in Concrete. *J. Mater. Civ. Eng.* **2019**, *31*, 04019307. [CrossRef]
39. Jeon, I.K.; Qudoos, A.; Woo, B.H.; Yoo, D.H.; Kim, H.G. Effects of Nano-Silica and Reactive Magnesia on the Microstructure and Durability Performance of Underwater Concrete. *Powder Technol.* **2022**, *398*, 116976. [CrossRef]
40. Wang, L.; Chen, L.; Tsang, D.C.W.; Guo, B.; Yang, J.; Shen, Z.; Hou, D.; Ok, Y.S.; Poon, C.S. Biochar as Green Additives in Cement-Based Composites with Carbon Dioxide Curing. *J. Clean. Prod.* **2020**, *258*, 120678. [CrossRef]
41. Meena, A.; Parikh, T.; Singh Gupta, S.; Serajuddin, A.T.M. Investigation of Thermal and Viscoelastic Properties of Polymers Relevant to Hot Melt Extrusion-II: Cellulosic Polymers. *J. Excip. Food Chem.* **2016**, *5*, 1–10.
42. Mohammed, A.M.A.; Yunus, N.Z.M.; Hezmi, M.A.; Rashid, A.S.A. Sequestration of Carbon Dioxide Using Ground Granulated Blast Furnaces Slag and Kaolin Mixtures. *Glob. Nest J.* **2021**, *23*, 105–111. [CrossRef]

43. Siriruang, C.; Toochinda, P.; Julnipitawong, P.; Tangtermsirikul, S. CO_2 Capture Using Fly Ash from Coal Fired Power Plant and Applications of CO_2-Captured Fly Ash as a Mineral Admixture for Concrete. *J. Environ. Manag.* **2016**, *170*, 70–78. [CrossRef]
44. Zhao, H.; Xiao, Q.; Huang, D.; Zhang, S. Influence of Pore Structure on Compressive Strength of Cement Mortar. *Sci. World J.* **2014**, *2014*, 247058. [CrossRef] [PubMed]